Histological, immunohistochemical and genetic study on the impact of endothelial progenitor cells in rat' pressure ulcer healing and angiogenesis with forensic evaluation of wound vitality.

Abstract:
Background: pressure ulceration (PU) is a thought-provoking complication of ischemia followed by reperfusion characterized by high disability, mortality and morbidity. Vitality of wounds remains a major challenge in forensic medicine especially in the context of suspected neglect or abuse. Bone marrow-derived endotheliaI progenitor cells (EPCs) usage has been broadly manipulated in diabetic wound patients owing to its high contented angiogenic and growth factors.
Aim: To assess the efficacy of EPCs therapy in promoting PU healing in relation to angiogenesis and epidermal cells regeneration based on histological, immunohistochemical and molecular mechanisms, and to explore its potential relevance as a supportive experimental model for studying wound vitality in pressure-related skin injuries.
Methods: thirty adult albino rats were assigned to 3 groups [control, PU and EPCs + PU groups]. Combines of two magnets were applied to the skin on the backs of rats to instigate ischemia followed by reperfusion. Histological and immunohistochemical analysis performed on the 14th day of the experiment. The effect was evaluated by assessing dermic collagen by Masson trichrome stain, re-epithelialization by PCNA immunostaining and angiogenesis by CD31 immunostaining. Gene expression of MMP, TIMP VEGF and VWF gene expression were also evaluated.
Results: Better wound restoring of EPCs+PU group compared to PU group after 14 days as EPCs initiated re-epithelialization, angiogenesis, a significant collagen area expansion and help epidermal cells regeneration. These findings may contribute to understanding the characteristics of vital wound healing in pressure-related skin injuries and could support future forensic investigations.
Keywords: pressure ulcer, endothelial progenitor cells, angiogenesis, wound vitality.

.

Introduction

A pressure ulcer (PU) or decubitus ulcer, is the end outcome of prolonged ischemia subsequently reperfusion usually with friction above a bony prominence [1]. The aged and immobile people are more impressionable to PU complications. Decreased serum albumin degrees,

diabetes, dietary insufficiency, low blood pressure and incontinence are leading causes to PU [2].

In Egypt, PU prevalence was registered 17.5% in 2020 with a global incidence in public hospitals of 9.2% [3]. The cost of PU patients reaches $80,000 In the USA, so researchers focused on studying the PU pathophysiology to spot on new therapeutic treatment lines [4]. The classification of PU depends on pathological picture is four stages starting from stage I with a picture of closed wound [5]. Stage II follows epidermal breaking down, so dermis promptly loses collagen fibers, inflammatory cells infiltration and amplifies risk of infection [6]. stage III , the wound is complicated into full thickness ulcer and wound, with muscle exposer. In stage IV, the wound becomes worthen exposing the bone with massive necrosis [7].
Bone marrow- stemmed endothelial progenitor cells (EPCs) performance as a prominent participant in angiogenesis and preserving function and cellular structure of vascular endothelium, as they can differentiate into endothelial cells in response to tissue ischemia so, they migrate to new blood vessels formation in response to several cytokines [8]. Foot lacerations particularly in peripheral arterial disease patients exhibited diminished EPC concentrations in countless studies with vascular complication [9]. The improvement of blood flow in wound healing is alleviated in many studies of ischemic ulcer but the role of EPCs not distinguished [10].

Gene's expression of wound healing genes has important role in diminished inflammation and regeneration as they conveyed to the procedure of ulcer healing [11]. Matrix metalloproteinases (MMPs) are a family of zinc-dependent endopeptidases comprising more than 20 members identified across multiple mammalian species, where they play essential roles in extracellular matrix remodeling, tissue repair, angiogenesis, and wound healing." [12]. The proteoIytic activity of MMPs is controlled by inhibitory proteins known as tissue inhibitors of metaIloproteinases (TIMPs) [13]. Four types of TIMP molecules—TIMP-1, -2, -3,4 can block all MMPs. TIMPs attach temporarily to the active part of MMPs in a one-to-one ratio. [14].

Vascular endothelial growth factor (VEGF) is responsible for starting the process of making further blood vessels, in away helps provide nutrients to the developing tissue. It also helps rebuild the outer layer of tissues, called the extracellular matrix, by creating proteins like proteoglycans,

collagen III, elastin, and laminin [15]. In the later stage, which can last for months or even years, the extracellular matrix slowly breaks down. During this time, type one collagen substitutes type three collagen and the collagen threads in the skin are rearranged. This process is carefully controlled by enzymes called matrix metalloproteinases (MMPs) and their inhibitors (TIMPs), which also influence how cells die and how new cells develop [16].

The plasma gIycoprotein von WilIebrand factor (VWF) is primarily synthesized by endothelial cells and megakayocytes and stored in Weibel–Palade bodies and platelet α-granules. Beyond its established role in hemostasis, vWF may indirectly influence inflammatory cell recruitment through interactions with endothelial cells, platelets, and the vascular microenvironment." [17].

von Willebrand factor (vWF) plays an important role in vascular homeostasis and hemostasis. In addition to mediating platelet adhesion and thrombus formation, vWF contributes to inflammatory responses by facilitating leukocyte rolling, adhesion, and transmigration across the endothelium. Furthermore, vWF has been implicated in vascular remodeling by influencing smooth muscle cell proliferation and regulating angiogenesis [18].

Recently, immunohistochemistry, biochemistry, and molecular biology have been introduced in the field of lesion vitality and age demonstration in which conduct the study in wound vitality and confirm that the injury occurrence during life may be neglected or delayed treated in case the healing is abnormal or complicated by infection [47]. The assessment of wound vitality at approximately 14 days post-injury may provide supportive evidence that the injury occurred during life. Abnormal healing patterns, especially when associated with infection, may also raise suspicion of neglect or delayed medical care. In addition, molecular and histopathological markers may enhance the accuracy and reliability of wound evaluation in medicolegal practice. However, these findings should be interpreted cautiously, as the current study did not include postmortem wound models or direct comparison between antemortem and postmortem injuries.

Aim of the work

To assess the efficacy of EPCs therapy in promoting PU healing in relation to angiogenesis and epidermal cells regeneration based on histological, immunohistochemical and genetic evaluations, and to investigate its potential relevance to the forensic assessment of vitality in pressure-related skin injuries.

Materials and methods

Experimental animals

AduIt male albino rats, which are 6 weeks old and weight between 180 and 200 grams, were achieved from the Experimental Animal Unit at the Faculty of Veterinary Medicine in Benha University, Egypt. The rats were raised and kept in a climate-controlled animal facility under special conditions that prevent the presence of harmful pathogens. All the rats were kept in uncontaminated cages and provided with a standard diet and clean water whenever they wanted. The rats lived in a normal sunlit and dark schedule and a room temperature of around 23 degrees Celsius, plus or minus 3 degrees. They could eat as much regular food and drink as they wanted. This study was done carefully the Guide for the Care and Use of laboratory Animals, published by the National Institutes of Health (NIH publication No. 85–23, revised 2011), which outlines the principles and practices that must be followed to ensure the human treatment of animals used in research (RC-2023).

Pressure ulcer induction

A subcutaneous injection of buprenorphine at a dosage of 0.01 – 0.05 mg/kg every cycle of ischemia [51] helped relieve pain in that stage. Rats backs were shaved by surgical scalpel. The backs were subsequently cleaned with warm, damp cotton pad. The skin was softly stretched, and the magnets (which are silver-coated neodumium magnets, model FZ6576S, with a thickness of 12 mm and thickness of 2 mm, measuring 2000 Gauss strength, N42 grade, from Magnet Specialist Therapy Magnets in the USA) were placed on the skin, departing one cm space between the skin and the magnets [19]. The rats were put back into cages that aren't magnetic and given time to heal. After 12 hours without blood flow, the magnets were taken for 12 hours away, so that blood could flow back again and that cycle of ischemia- reperfusion done for seven days. Skin that was irritated and had a small area of untouched skin was saved on the 14^{th} day of the experiment.

Experimental design and protocol.

The experimental design as thirty adult male rats were randomly and equally divided into three groups as follows:

Group I (control group, unwounded group): The rats were separated equally into 2 subgroups:

Subgroup Ia: The rats were placed without intervention.

Subgroup Ib: The rats were injected by normal saline via tail vein.

Group II (pressure ulcer): Rats were subjected to magnets inducing PU for 7 days.
Group III (pressure ulcer + EPCs): Rats were subjected to magnets inducing PU for 7 days and at the same time, then the rats received EPCs transplantation within the tail vein (4.5 × 10^5 cells/rat). The transplantation repeated for 2 times three days apart.

Isolation of mononuclear cells.
We measured the number of EPC- the same as mononuclear cells in the bone marrow in the central lab of benha faculity of medicine. The bone marrow cells of the donor rats could be collected by flushing the bone marrow cavity per heparinized saline. BM- mononuclear cells were separated by spinning the sample across a Histopaque-1099 density grade, which was obtained from Sigma, UK. Cells were saved and placed on 100-mm plastic dishes that were coated with 2% gelatin [20].

Primary culture of rat BM- EPCs
The isolated bone marrow endothelial progenitor cells (BM-EPCs) were propagated in Dulbicco's Modefied Eagle Medium (DMEM) (Sigma-UK) comprising 10% fetal bovene serum (FBS) (Bio-west, Cail1e, Frances) and P-S solution (Sigma- UK) [21].

EPCs culturing
In the cell culture, cell growth stimulation was done by medium 166 comprising 25% FBS (Bio-west), bovid pituitary extracts (Bio-medical MAO, USA) with antibiotics (Gibco) [22]. The development completed in the seventh day of culture via attached cells [21].

Flow cytometry & Cell labeling.
On day 7 of the culture, five samples of endothelial progenitor cells were analyzed using flow cytometry with a FACS Scan fIow cytometer from Becton-Dickinson in California, USA. Dead cells were removed using propidium iodide (from Sigma). The EPCs were first washed, then treated with an FcR blocking reagent from Miltenyi Biotec in California, USA. After that, they were incubated with primary antibodies for 35 minutes at 4°C. CD45,VEGFR2 and CD31 were the primary antibodies used (Becton-Dickinson) (Abcom, Cambridge, UK) [23]. Labeling of cultured cells in skin samples were done by red fluorescent dye, PKH-26-red (Sigma, USA) for EPCs detection in transplanted skin [24].

Sampling
Rats in each group were sacrificed following 14 days PU initiation. Samples were acquired from the middle-injured area. Hemi skin tissues

were examined under a microscope using hematoxyIn and eosin (H&E) and Masson's trichrome stains. Immunohistochemical tests for PCNA and CD31 were additionally carried out. The remaining half of the skin tissue samples were freezing at minus 80 degrees Celsius for later use in quantitative real-time polymerase chain reaction (qRT-PCR) to check gene levels expression of MMP, TIMP VEGF and vWF.

Histological analysis

The first half skin tissue in all groups was placed in 10% buffered formal saline, then embedded in paraffin, and cut into thin sections of 4.0 micrometers. These sections were treated with increasing intensities of ethanol to remove moisture and rinsed twice in distilled water. For the skin samples from the 14^{th} day, the tissues were stained with hematoxyIin and eosin (H&E) to examine re-epithelialization and connective tissue progression, and Masson's trichrome to assess collagen buildup, following the manufacturer's recommendations. The stained tissue slides were then examined and evaluated per a microscope (Leicaa DMRR 3000; Leica, Microsystems) by experienced researchers who were unaware of which group the samples came from. [25].

Immunohistochemical staining

To detect new blood vessel creation in the ulcer area, the tissue samples were examined using a CD31- primary antibody (rabbit monoclonaI, SAR5500069, Sigma, USA). To identify the proliferation of basal keratinocytes, a PCNA primary antibody was consumed (rabbit polyclonal Anti-Proliferating Cell Nuclear Antigen antibody, SAR2701019, Sigma, USA).

After the tissue was fixed, embedded in paraffin later dewaxed, the sections were hindered using a solution containing 4% normal goat serum, 0.4% Triton X-100 lastly 0.1% BSA (all from Sigma) within PBS. The sections were subsequently incubated pro 24 hours at 3°C with the respective primary antibodies (CD31 and PCNA) at a 1:100 dilution. Following this, the sections were incubated for 1.5 hours at room temperature with the subsequent secondary antibody, goat anti-mouse IgG. After staining with hematoxylin, the tissue sections were processed to washing later dehydrated consuming ethanol, cured with dimethylbenzene, and then potted for microscopic examination by experienced examiners who were blinded to the study details. The positive control for CD31 and PCNA staining were of liver and tonsil

sections respectively while negative control sections were achieved by eliminating the primary antibody [26].

Morphometric study

The average area percentage per collagen fiber buildup, as shown by Masson's trichrome slides, the average area percentage of PCNA, and the count of CD31-positive blood vessels were measured to assess new blood vessel formation. These measurements were taken from five images, each from a different non-overlapping area in every rat from each group, managing the Image-G-Pro Plus software version 9.0 (Media Cybernentics Inc., Betheshda, Maeryland, USA).

Statistical analysis

A statistical examination was conducted utilizing the SPSS version 26 program on my computer system (Chicago, Illinois, United States. Version 8 of GraphPad's popular statistical software program) utilized for visualizing data graphically. The differences among group samples were analyzed through an ANOVA conducted initially; subsequently, post hoc comparisons employed. The data is presented using means along with their associated standard errors (SEM; parametric methods) and medians (non-parametric techniques); Spearman correlation coefficients have been calculated to assess relationships among various factors; statistical significance was determined by evaluating p values less than 0.5% [52].

Gene Expression Analysis

Total RNA was extracted from wound fluid samples using Invitrogen TRIzol reagent according to the manufacturer’s instructions. RNA concentration and purity were determined using a Thermo Fisher Scientific NanoDrop 2000/2000c spectrophotometer by measuring absorbance at 260 and 280 nm. All RNA samples demonstrated acceptable purity, with A260/A280 ratios greater than 1.9.

Complementary DNA (cDNA) was synthesized from total RNA using the QIAGEN QuantiTect Reverse Transcription Kit according to the manufacturer’s protocol. Synthesized cDNA was stored at −20°C until further analysis.

The relative mRNA expression levels of VEGF, vWF, MMP-3, and TIMP-1 were quantified by real-time quantitative PCR (qRT-PCR). GAPDH was used as the internal housekeeping gene for normalization due to its stable expression across all experimental groups.

Each biological sample was analyzed in triplicate technical replicates to ensure reproducibility. Each experimental group consisted of 10 independent biological samples (n = 10).

PCR amplification was performed under the following conditions: initial denaturation at 95°C for 2 min, followed by 40 cycles of denaturation at 95°C for 15 s, annealing at 60°C for 30 s, and extension at 72°C for 30 s, with a final extension at 72°C for 9 min.

Melting curve analysis was performed following amplification to confirm product specificity and exclude nonspecific amplification or primer-dimer formation.

Relative gene expression was calculated using the 2−ΔΔCt method after normalization of target gene Ct values to GAPDH, with the control group serving as the calibrator.

Primer sequences (5′–3′)

Gene	Forward Primer	Reverse Primer
VEGF	**CACTGGACCCTGGCTTTACT**	**GACGTCCATGAACTTCACCA**
vWF	**CGGCTTGCACCATTCAGCTA**	**TGCAGAAGTGAGTATCACAGCCATC**
MMP-3	**TGGAGATGCTCACTTTGACGA**	**CCTTGGCTGAGTGGTAGAGTC**
TIMP-1	**CCAGAGCCGTCACTTTGCTT**	**AGGAAAAGTAGACAGTGTTCAGGCT**
GAPDH	**GCCCCTTCTGCCGATGC**	**CTTTCCAGAGGGGCCATCC**

Results

Identification of BM-EPCs. After seven days in culture, the exo vivo expanded EPCs that were assigned to the surface showed positive results for CD31 (62.1 _ 6.1%) and VEGFR2 (7.1 _ 6.6%) but not for CD45 (3.4 _ 0.98%) which is an indicator for leukocytes (Fig. 1a). Endothelial progenitor cells stamped through red fluorescence were seen in skin specimen from group III (Fig. 1b).

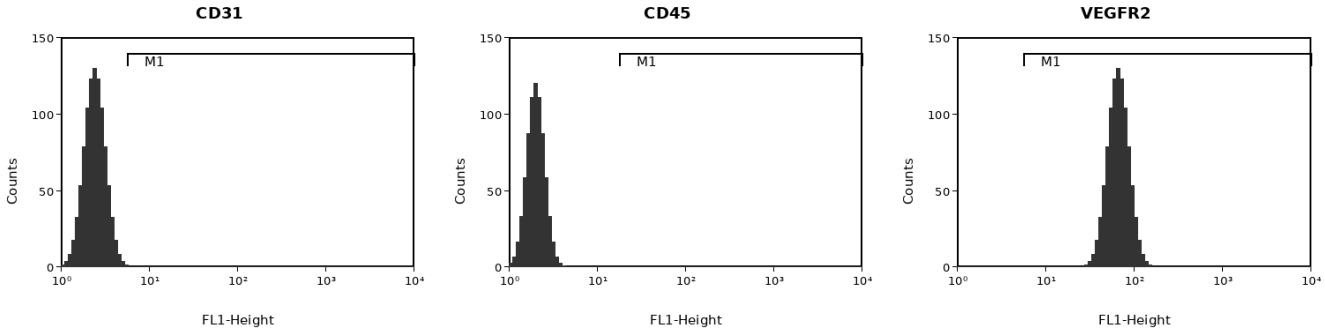

CD31 — Negative (single dim peak)

CD45 — Negative (single dim peak)

VEGFR2 — Positive (right-shifted peak in M1)

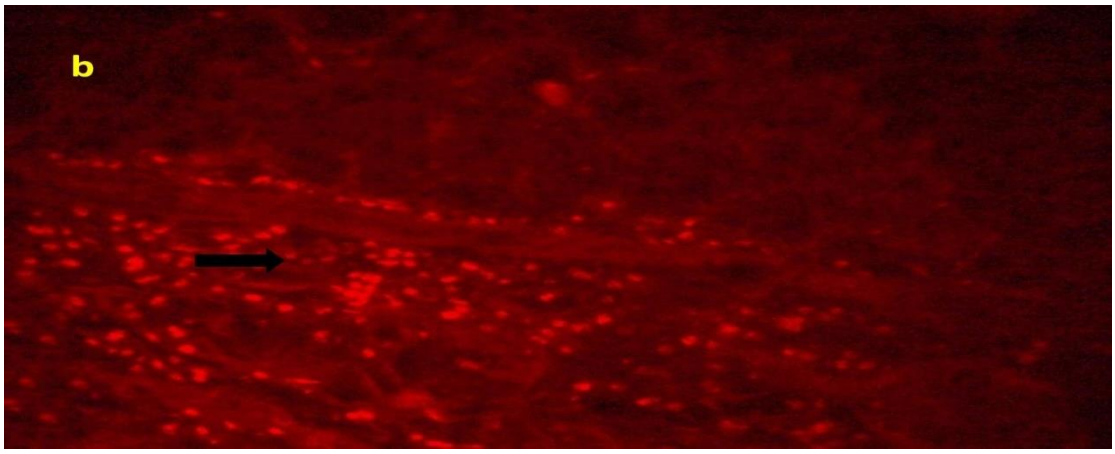

Fig. 1: Characterization of cultured BM-derived EPC. (a) Flow cytometry showed developed EPC that were positive for CD31 (62.1 _ 6.1%) but not for CD45 (3.4 _ 0.98%) (b) A fluorescent microscope image displaying endothelial progenitor cells that have been labeled with the PKH26 fluorescent dye in skin tissue (arrow).

H&E results

The control group stained by H&E showed the normal histological structure in thin skin. The epidermis is arranged in a keratinized stratified squamous epithelium, mostly comprising keratinocytes settled in four strata: Stratum Basale, Stratum spinosum, Stratum granulosum and covered with Stratum corneum as lamellated keratin scales. The dermis was established of two layers. The superficial layer, called the papillary layer, had thin, crisscrossing collagen fibers, some connective tissue cells, and many small blood vessels. The deeper layer, known as the reticular layer, was thicker what is more not clearly separated from the papillary layer. It had fewer cells and was made up of thicker collagen strands that went in various directions, with some scattered hair follicles in there. (Fig. 2a).

The PU group (group II) showed an ulcer bed which is enveloped with a single sheet of squamous cells with notable discontinuation of the

covering keratin layer. The epidermis upon both sides the ulcer beds seemed thin beside disorganized keratinocytes; some appeared vacuolated & others showed deeply stained pyknotic nuclei. The papillary layer was deficient in blood capillaries, whilst the reticular layer was disrupted in hair follicles. The dermis showed many inflammatory cellular infiltrates within the disorganized collagen with scattered areas of lacking collagen deposition (Fig. 2b).

Examination of the EPCs-treated group showed intact thin skin. The epidermis had more or less thickness of control group, regular and covered with a continuous well-arranged keratin layer. The dermis is formed of the known layers: the papillary layer with scattered blood capillaries and the reticular layer with numerous hair follicles and well-organized thick collagen bundles (Fig.2c).

Masson's trichrome results:

The control group dermal collagen appeared fine, interconnecting fibers inside the papillary layer, and as crowded, wavy, densely packed blue bundles in the reticular layer. (Fig. 3a). The PU group showed a clear reduction in collagen in both the papillary and reticular layers. In both layers, the collagen fibers were loosely arranged with noticeable spaces between them. Some areas had little to no collagen deposited. However, a few regions displayed thick clusters of collagen bundles. (Fig. 3b). Alternatively, the EPCs groups exhibited a gradual intensification in fine collagen fiber deposition in the papillary layer, along with better organization of the thick collagen bundles in the reticular layer, which were arranged in different directions compared to the PU group. (Fig. 3c).

Anti-PCNA Immunohistochemical staining:

Immunohistochemical staining using an anti-PCNA antibody was done to check how fast cells proliferation in the skin area of the ulcer. In group I, many cells in the lowest layer of the skin cells showed a strong nuclear reaction (Fig. 4a). However, in the PU group, the reaction was much weaker in the lowest layer of the skin cells nuclei (Fig. 4b). In the EPCs groups, the reaction strength in skin cells nuclei was more similar to that seen in group I (Fig. 4c).

Immunohistochemical detection of angiogenesis:

The formation of new capillaries was checked using the CD31 marker. In the control group, there was a moderate level of CD31 expression in the capillaries of the papillary layer of the dermis (Fig. 5a). In the PU group, CD31 staining coexisted sparse (Fig. 5b). However, the EPCs groups showed more new vessel (Fig. 5c).

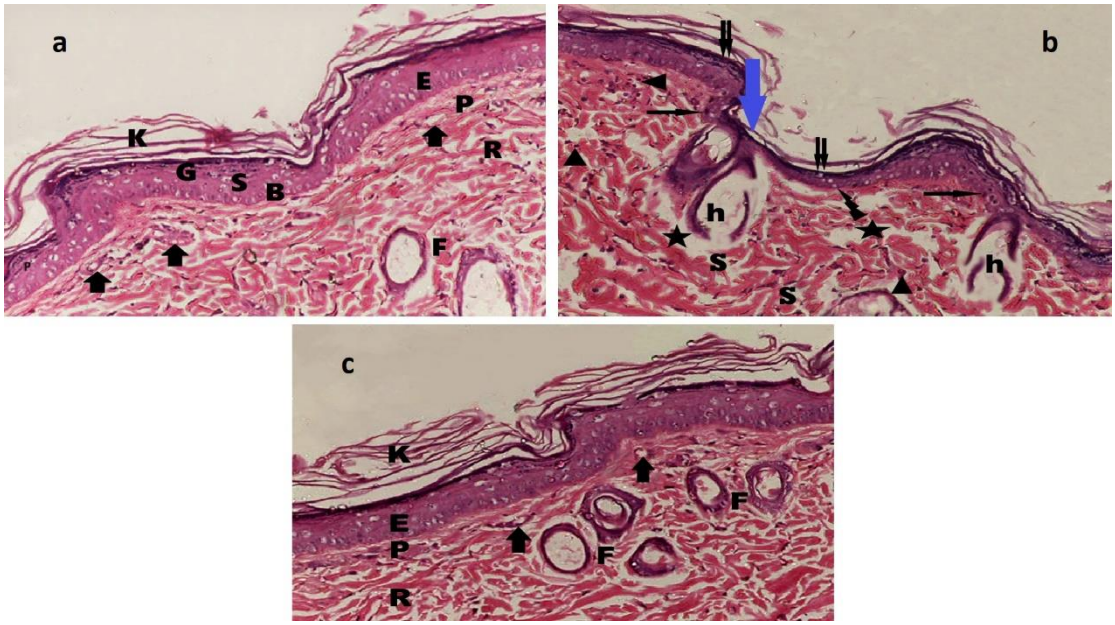

Fig. (2): photomicrograph of H&E stained sections from rats thin skin in different experimental groups: (a) control group revealing the epidermis layer (E) shows a stratified squamous keratinized epithelium, comprising keratinocytes arranged in 4 strata: Stratum Basale (B), Stratum spinosum (S), Stratum granulosum (G) and covered with Stratum corneum as lamellated keratin scales (K). The dermis shows a superficial papillary layer with thin interlacing collagen fibers (P) and numerous blood capillaries (arrow). The deeper reticular layer containing thick collagen bundles (R) and scattered hair follicles (F). **(b)** PU group showing an ulcer bed (blue arrow) which is covered by a single layer of squamous cells with notable discontinuation of keratin layer. The epidermis on either side of the ulcer beds appears thin (double arrow) with disorganized keratinocytes; some appear vacuolated (zigzag arrow) & others show deeply stained pyknotic nuclei (arrow). The dermis showing many inflammatory cellular infiltrations (head arrow) and marked spacing in-between the loosely arranged collagen fibers (S) with some areas deficient of collagen (star). Notice, damaged hair follicles are seen (h). (**C**) the EPCs-treated group showing apparently intact thin skin. The epidermis (E) appears regular and covered with a continuous well-arranged keratin layer (K). The dermis is formed of the known layers, the papillary layer (P) with scattered blood capillaries (arrow) and the reticular layer (R) with numerous hair follicles (F). (**H&E X400)**

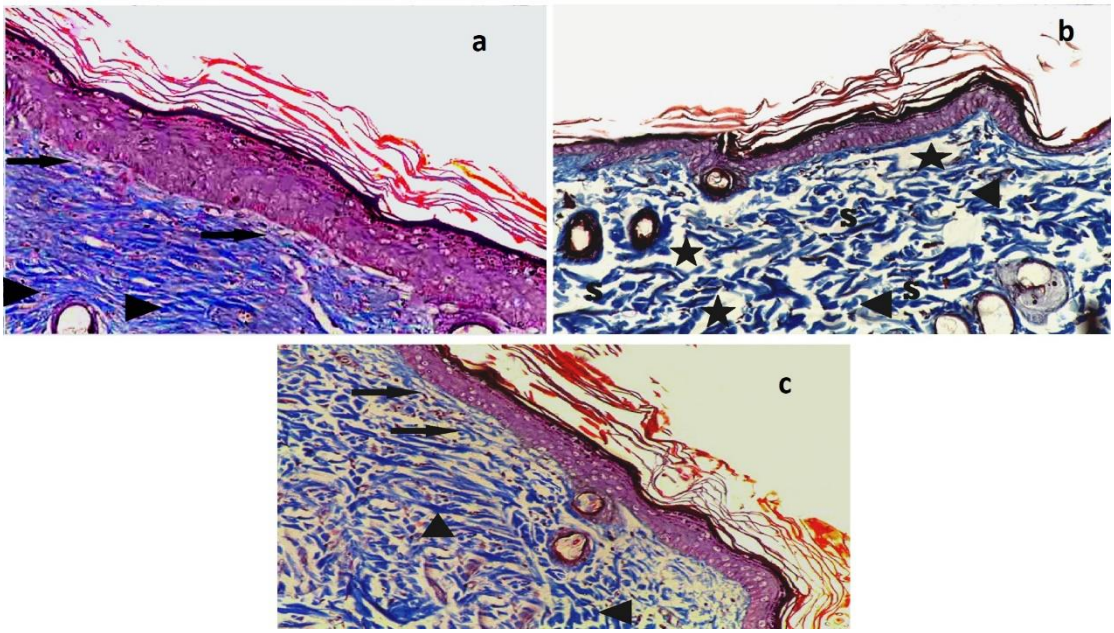

Fig 3: Representative photomicrographs of Masson's trichrome stained skin sections:
(a) The control group showing the normal distribution of the dermal collagen fibers; fine interweaving fibers in the papillary layer (arrow), and thick, wavy, densely packed blue bundles in the reticular layer running in different directions (head arrow)**. (b)** The PU group reveals an obvious decrease in collagen in the papillary and reticular layers. Both layers show loosely arranged collagen fibers and marked spacing in-between (S) with some areas deficient of collagen (star). Notice, dispersed thick irregular collagen bundles (head arrow). **(C)** EPCs group shows a progressive rise in fine collagen fiber deposition in the papillary layer (arrow) thru improvement in the configuration of the thick collagen bundles which run in different directions in the reticular layer (head arrow) compared to the PU group (Fig. 3c). **(Masson trichrome X400).**

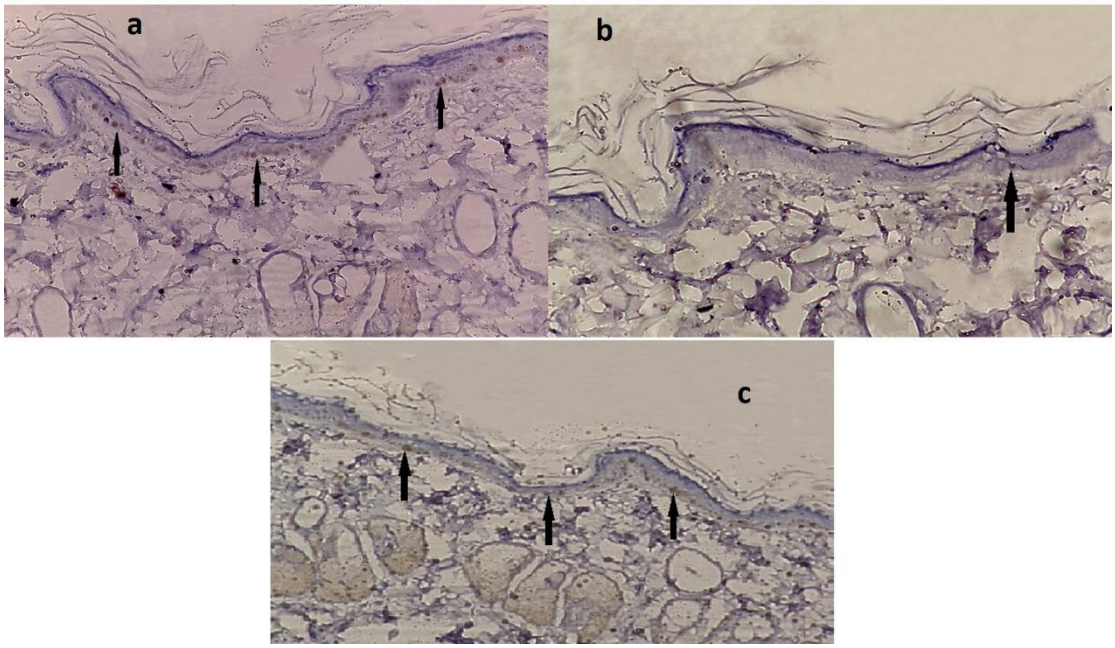

Fig 4: Representative photomicrographs of Anti-PCNA Immunostained skin sections:
(a) The control group shows an intense reaction in cells of the basal keratinocytes layer of, whereas **(b)** in PU group, there was a weak reaction in the basal keratinocytes layer. **(c)** In the EPCs groups, the intensity of the reaction keratinocytes intensified comparable to the PU group. **(**Anti-PCNA **Immunostain X400).**

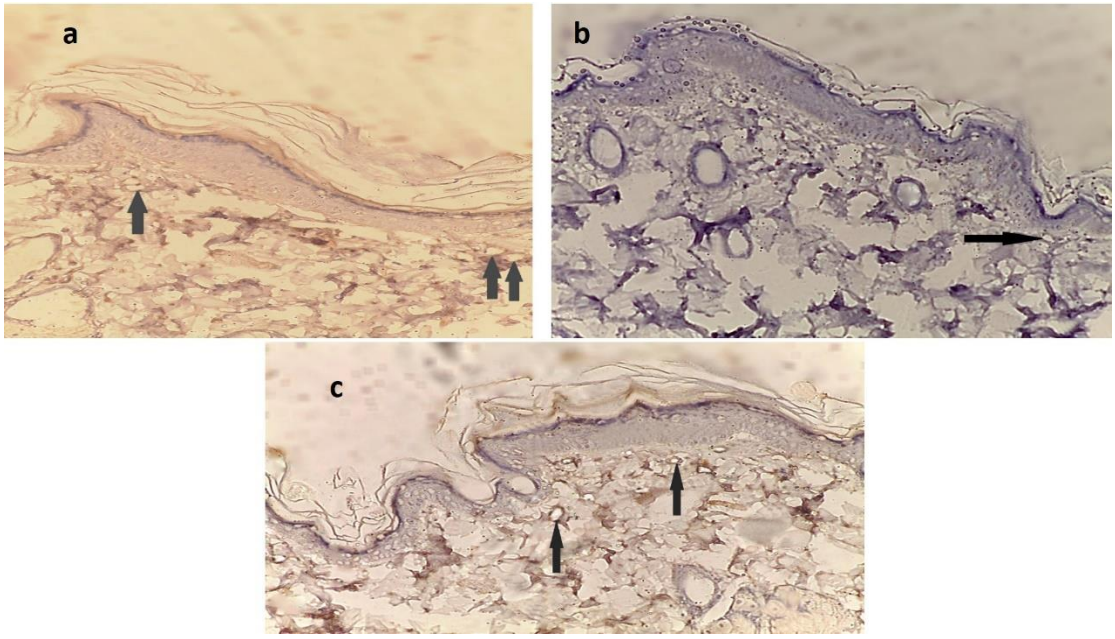

Fig 5: Representative pictures of anti cd31 immunostained skin sections:
(a) In the control group, a moderate cd31 expression expresses in the capillaries of the papillary layer of the dermis. **(b)** In the PU group, a rare cd31 reaction is seen. **(c)** On the other hand, the EPCs groups show increasing new vessel formation. **(Anti cd31 Immunostain X400).**

Morphometric results

In sections stained with Masson trichrome, the average area percentage of collagen in the dermis existed 23.2 ± 1.0% inside the control group. The PU group showed a significantly lower collagen level, at 13.1 ± 0.3%, compared to the control group ($p < 0.05$). EPCs treated group, a significant increase in collagen sedimentation detected. The healed groups had an average collagen area percentage of 22.5 ± 0.5%, which was significantly near like the control group ($p < 0.05$) (histogram 1).

In the sections stained for anti-PCNA, the average area covered by anti-PCNA coexisted 1.3 ± 0.0% concerning the control group. In the PU group, the average area covered by anti-PCNA dropped significantly to 0.1 ± 0.0% compared to the control group ($p < 0.05$). After therapy with EPCs, the average area covered by anti-PCNA increased back to 1.6 ± 0.0%, which was significantly higher than the control group ($p < 0.05$) (histogram 2).

Morphometric analysis of cd31expression showed in the control group, the count of CD31-positive capillaries was (3.4 ± 0.2). The PU group showed a signlficant drop in capillary count, measuring (0.1 ± 0.0), in away lower than the control group ($p < 0.05$). Later on treatment with EPCs, the CD31-positive count increased significantly to (5.9 ± 0.8), which stayed higher than the control group ($p < 0.05$) (histogram 3).

Histogram 1: The mean area% of positive collagen for Masson trichrome in all groups.

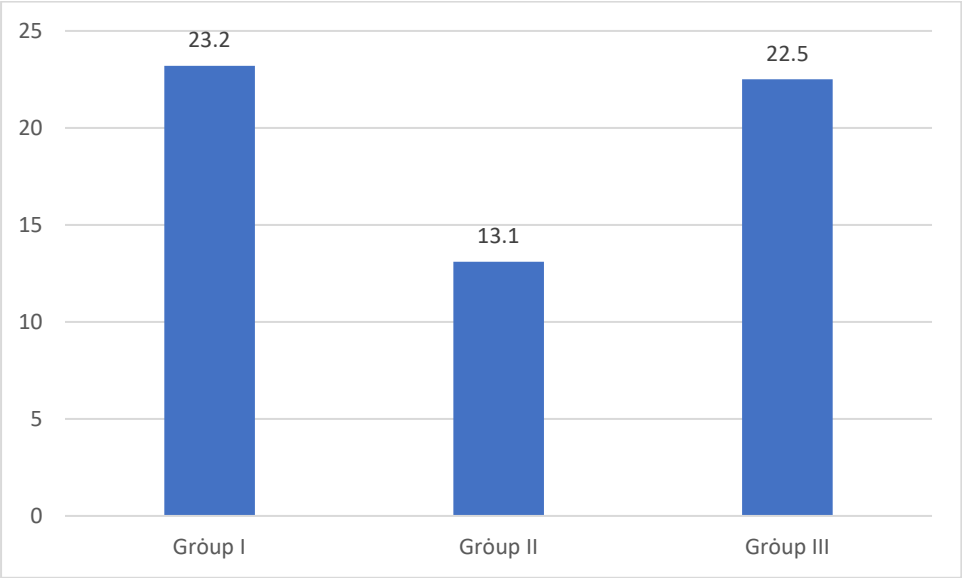

Histogram 2: The mean area% of positive immunoreactive reaction for anti-PCNA in all groups.

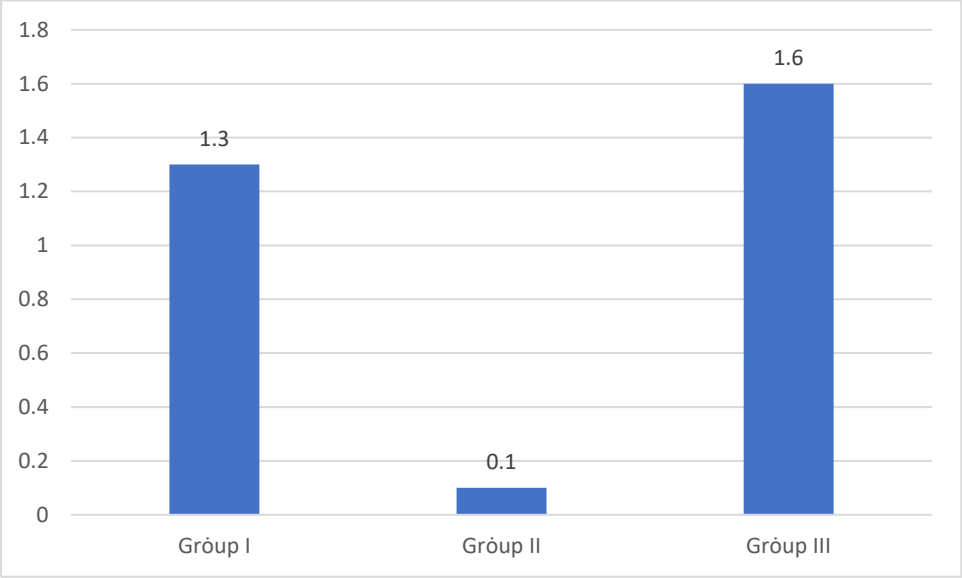

Histogram 3: The mean sum of positive immunoreactive cells for the count of CD31-positive capillaries in all groups.

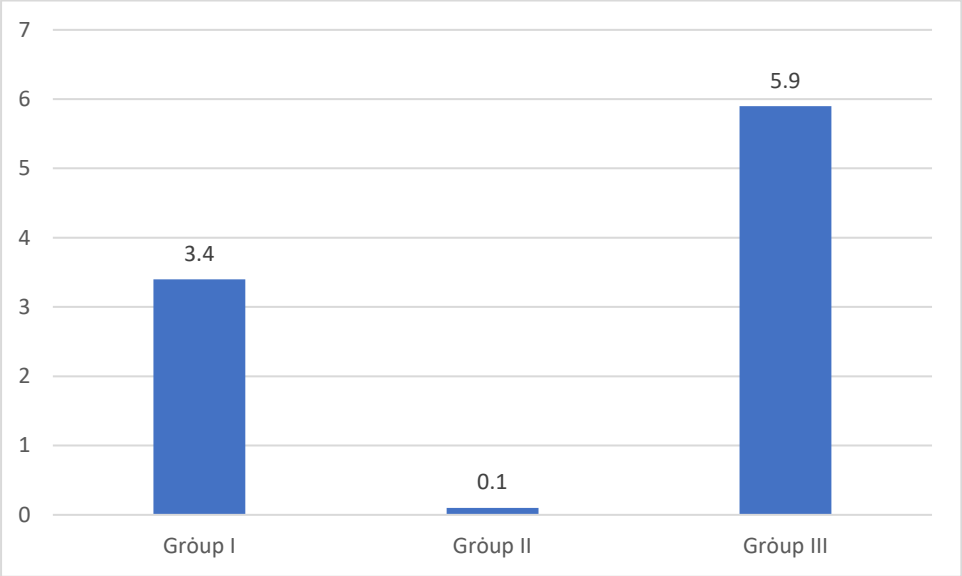

Gene's expression results:

Table (1): MMP3 gene expression between examined groups.

		Group 1 Control (N=10)	Group 2 (N=10)	Group 3 (N=10)	Test value	P-value
MMP 3	**Median (IQR)**	1 (1-1)	126.873 (125.962- 128.439)	55.418 (53.439- 55.963)	Kw = 26.76	**<0.001** P1<0.001 P2=0.029 P3=0.029**
	Range	1-1	120.312 - 130.875	50.612- 58.895		

p>0.05 is statistically non-significant, *p≤0.05 is significant, **p≤0.01 is high significant,
Kw: Kruskal Wallis Test. P1: P-value in group 1 & 2, P2: P-value in group 1 &3, P3: P-value in group 2 & 3

The median (IQR) **MMP3** level in group 2 was 126.873 (125.962-128.439) while its level in group 3, was 55.418 (53.439- 55.963. **MMP3** level was significantly downregulated in group 3 compared to group 2 (p<0.001). In addition, groups 2& 3 were significantly higher than control (group 1).

Table (2): TIMP1. gene expression between reviewed groups

		Group 1 Control (N=10)	Group 2 (N=10)	Group 3 (N=10)	Test value	P-value
TIMP1 P	**Median (IQR)**	1 (1-1)	27.914 (26.612- 28.778)	89.928 (88.434-90.479)	Kw = 26.79	**<0.001** P1<0.001 P2=0.02**
	Range	1-1	25.963 - 29.863	80.781- 92.993		

						9 P3=0.029

p>0.05 is statistically non-significant, *p≤0.05 is significant, **p≤0.01 is high significant, Kw: Kruskal Wallis Test. P1: P-value in group 1 & 2, P2: P-value in group 1 &3, P3: P-value in group 2 & 3

The median (IQR) **TIMP1** level in group 2 was 27.914 (26.612- 28.778) while its level in group 3, was 89.928 (88.434-90.479). **TIMP1** level was significantly higher in group 3 compared to group 2 (p<0.001). In addition, both groups 2& 3 were significantly higher than control (group 1).

Table (3): Von Willebrand factor gene expression between considered groups

		Group 1 Control (N=10)	**Group 2 (N=10)**	**Group 3 (N=10)**	**Test value**	**P-value**
Von Willebrand factor	**Median (IQR)**	1 (1-1)	96.329 (97.863- 92.781)	32.109 (29.933-32.974)	Kw = 26.79	**<0.001** P1<0.001 P2=0.029 P3=0.029**
	Range	1-1	92.781 -99.479	27.612 -33.963		

p>0.05 is statistically non-significant, *p≤0.05 is significant, **p≤0.01 is high significant, Kw: Kruskal Wallis Test. P1: P-value in group 1 & 2, P2: P-value in group 1 &3, P3: P-value in group 2 & 3

The median (IQR) **Von Willebrand factor** level in group 2 was 96.329 (97.863-92.781) while its level in group 3, was 32.109 (29.933-32.974). **Von Willebrand factor** level was significantly lesser in group 3 compared to group 2 (p<0.001). In addition, groups 2& 3 were significantly higher than control (group 1).

Table (4): vascular endothelial growth factor gene expression between planned groups

		Group 1 Control (N=10)	**Group 2 (N=10)**	**Group 3 (N=10)**	**Test value**	**P-value**
Vascular endothelial growth factor	**Median (IQR)**	1 (1-1)	22.737 (20.895 - 23.439)	94.236 (91.781 - 95.993)	Kw = 26.79	**<0.001** P1<0.001 P2=0.029 P3=0.029**
	Range	1-1	19.963 - 25.711	90.665 - 96.743		

p>0.05 is statistically non-significant, *p≤0.05 is significant, **p≤0.01 is high significant, Kw: Kruskal Wallis Test. P1: P-value in group 1 & 2, P2: P-value in group 1 &3, P3: P-value in group 2 & 3.

The median (IQR) **vascular endothelial growth factor** level in group 2 was 22.737 (20.895 - 23.439) while its level in group 3, was 94.236 (91.781 - 95.993). **Vascular endothelial growth factor** level occurred significantly elevated in group 3 compared to group 2 (p<0.001). Additionaly, its level in both groups 2& 3 was significantly higher than control (group 1).

Table (5): Spearman correlation between the different parameters among group 2.

		MMP	TIMMP	Von Willebrand factor	Vascular endothelial growth factor
MMP3	**ρ**		0.127	0.042	-0.176
	***P*-value**		0.726	0.907	0.627
TIMP1	**ρ**	.127		-0.212	0.479
	***P*-value**	.726		0.556	0.162
Von Willebrand factor	**ρ**	.042	-0.212		-0.055
	***P*-value**	.907	0.556		0.881
Vascular endothelial growth factor	**ρ**	-.176	0.479	-0.055	
	***P*-value**	.627	0.162	0.881	

P: Spearman correlation coefficient

Table (5) showed that there was no significant correlation was found between MMP3, TIMP1, Von Willebrand factor as well as Vascular endothelial growth factor in group 2.

Table 6. Spearman correlation analysis between studied markers

Variables	MMP-3 (ρ)	P-value	TIMP-1 (ρ)	P-value	vWF (ρ)	P-value	VEGF (ρ)	P-value
MMP-3	—	—	-0.079	0.829	0.345	0.328	0.406	0.406
TIMP-1	-0.079	0.829	—	—	-0.176	0.627	0.091	0.091
vWF	0.345	0.328	-0.176	0.627	—	—	0.539	0.539
VEGF	0.406	0.244*	0.091	0.803	0.539	0.108	—	—

P: Spearman correlation coefficient

Table (6) showed that there was no significant correlation was found between MMP3, TIMP1, Von Willebrand factor as well as Vascular endothelial growth factor in group 3.

Discussion:

There are still some issues that need to be addressed in the reconstruction of large-scale pressure sores, such as slow healing, noticeable scarring, and skin tightening, which are mainly due to the inability to properly regenerate blood vessel-rich skin tissue, leading to poorer results in repairing skin damage. [5]. Investigators have used ischemia and reperfusion by magnet in model type of pressure ulcer [19]. Magnet may aggravate injury which, triggered subdermal inflammation in skin caused by activated macrophages cytokines (TNF-α & IL-6) [27]. The lack of blood flow, resulting from a refusal -blood reflow phenomenon. In a

publication by [28] similar “no-reflow” was detected after 3h magnet usage in the rabbit’s limb by “plugs” in the form of blood cell aggregates. In certain parts of the skin within the affected area using a rat pattern of ischemia and reperfusion by [29], necro inflammatory debris started to build up. This is probably because neutrophils, gathered underneath the skin or an indication of epidermal necrosis 24 hours after the lack of blood flow.

In the present study assessment of group-II (pressure ulcer) H&E sections showed high damage in the epidermal and dermal skin stratums. These were coincided with [30] who mentioned that augmented inflammation triggered by pro-inflammatory cytokines, chemokines, reactive oxygen species, and proteolytic enzymes that are expressed in greater quantity due to injury by magnets. Contrary to that [31]**,** a Study has found that the subcutaneous connective tissue suffered significant damage, while the epidermis stayed undamaged during the magnet implantation process.

The papillary layer showed lack of blood capillaries, whereas the reticular Iayer showed disrupted hair follicles in PU group. This fell in accordance with [32], Who observed that endothelial cell growth was slowed and cell death was higher with severe harmful stimuli. Both layers of the dermis in the PU group showed many inflammatory cellular infiltrates this was in consistence with findings of [33] who found massive inflammatory infiltrate which vary according to the inflammatory phase of the ulcer; early acute inflammatory cells predominate, later chronic inflammatory cells if longer duration.

In the current study, the dermis of PU group exhibited collagen fibers reduction with loose arrangement and marked spacing in-between. Various areas deficient of collagen deposition while others exhibited heavy collagen bundles. This was explained by [34], who detected collagen degeneration and boundaries disappearing in middle fibers and ascribed this to water leaks from the tiny blood vessels called capillaries, leading to swelling and edema. This leakage also causes the collagen fibers to stick together and amalgamate.

Also, in PU group, there was a weak PCNA reaction in the basal cells of keratinocytes. [35] reported that the persistent inflammation decomposes the extra-cellular matrix stunted the re-epithelization. Similarly, the degraded growth factors may illuminate the significant drop in PCNA expression.

EPCs which are the precursor that develop into vascular endothelial cells which stimulates wide span of cytokines and growth factors that are essential target wound healing. These cells can grow, move, and turn into

different types of cells that line the inside of blood vessels. They can be found and collected from blood and spleen [24].
On histological observation of EPCs group, it exhibited accelerated reepithelization and increased keratinization in a favorable manner until ulcer repair. These findings are explained by [36] who mentioned the paracrine consequence of the EPCs via cytokines and growth factors, the increased epithelial cells proliferation and injury repairment. Also, EPCs migrate into the wound and enhance neovascularization ensuring adequate oxygen and nutrient delivery, which is essential to sustain cell growth and re-epithelialization.

Also, the EPCs groups exhibited a progressive rise in the collagen fiber deposition plus improvement in the organization of the collagen bundles of dermal stratum compared to PU group besides to control group. This was disagreed by [37] who reported considerable increased collagen fiber deposition in the wound tissues of EPC-treated group more than that of the control group. Authors of [38] explicated the stimulation effect of vascular endothelial cells in organization, maturation, deposition of collagen fibers and increased type III collagen assembly needed definitely in faster tissue repair.

Regarding PCNA expression, EPC-treated group, it was significantly enhanced and seems more than the control group. The increased intensity of PCNA reaction reflects that using EPCs indicates enhanced cell division and a higher rate of proliferation of keratinocytes in the basal layer, likely promoting epidermal regeneration and wound healing. [39] approved the higher epithelial cells proliferation rate found in BMSCs group, by amplified epithelial cells mitosis.

Moreover, we observed in the EPCs treated group, the strong stimulant effect that EPCs has by increased CD31 immunoreactivity in the dermal blood vessels (endothelial cells) compared to control group. In agreement with studies [40,41], who explained that, EPCs has stronger vascular regeneration ability both by direct differentiation to endothelial cells and via the paracrine actions of several growth factors, for instance VEGF-A, PDGF, VEGF-S and IGF-1,2 resulting in intense nutrition supply to the affected area and lessen the healing time.
.

In the present study, MMP 3 levels were significantly lower in group 3 compared to group 2 ($p < 0.001$), whereas TIMP-1 levels were significantly higher in group 3 compared to group 2. These findings suggest a shift toward reduced matrix degradation and enhanced

inhibitory control of matrix metalloproteinases during the later phase of healing. Previous studies have demonstrated that MMP-3 acts as an upstream activator of several pro-MMPs, positioning it as a key regulator in extracellular matrix (ECM) remodeling cascades, where it contributes to the degradation of ECM components including structural proteins, growth factors, receptors, and adhesion molecules (42). Excessive MMP activity, particularly when insufficiently regulated by TIMPs, has been implicated in chronic non-healing wounds due to persistent ECM breakdown. The TIMP family (TIMP-1 to TIMP-4) regulates MMP activity by binding to their catalytic domains, and an imbalance between MMPs and TIMPs is strongly associated with impaired wound healing and chronic inflammation.

Furthermore, MMPs and their inhibitors play a critical role in capillary morphogenesis and collagen organization during tissue repair. Dysregulation of this system may disrupt ECM remodeling and delay wound closure in chronic wounds characterized by sustained inflammation and elevated proteolytic activity (43,44).

In this study, vWF levels were significantly lower in group 3 compared to group 2 ($p < 0.001$). von Willebrand factor (vWF) is a key glycoprotein involved in hemostasis, platelet adhesion, and thrombus formation, and is widely recognized as a biomarker of endothelial dysfunction. Its expression is influenced by inflammatory and hypoxic stimuli, which promote endothelial activation and increased secretion (45,46). The reduced vWF expression in the EPC-treated group may represent reduced endothelial activation, decreased thrombotic activity, or progression toward vascular maturation during the later stages of wound healing, rather than endothelial dysfunction. This revised interpretation is more consistent with the concurrent increase in CD31 and VEGF, both of which support enhanced angiogenesis and vascular remodeling on the model context.

VEGF levels were significantly higher in group 3 compared to group 2 ($p < 0.001$). Vascular endothelial growth factor (VEGF) is a principal mediator of angiogenesis, with expression typically increasing following tissue injury to promote neovascularization and tissue regeneration. Elevated VEGF levels are associated with active granulation tissue formation, whereas reduced expression has been reported in delayed healing conditions such as diabetic foot ulcers (47). Together, these findings highlight a tightly regulated interaction between endothelial mediators (vWF, VEGF) and ECM-remodeling enzymes (MMPs/TIMPs)

in wound healing. Dysregulation of any of these components may impair angiogenesis, ECM remodeling, and overall tissue repair.

.

The findings of this study extend beyond therapeutic applications and may hold potential relevance in forensic medicine. The histological, immunohistochemical, and molecular changes observed during pressure ulcer healing—such as increased collagen deposition, neovascularization, and elevated expression of VEGF, vWF, MMP, and TIMP—may serve as supportive indicators associated with wound vitality. These findings reflect biological processes occurring in living tissue and may be considered as complementary evidence in forensic investigations.
Day 14 was selected for the wound vitality study as it represents an advanced stage of healing, where vitality-related markers and neovascularization are more clearly detectable. This stage may correspond to a late proliferative to early remodeling phase, characterized by relatively stabilized inflammatory and reparative processes. Accordingly, this time point may provide supportive information regarding whether the injury occurred during life and may help in understanding the progression of pressure-related skin injuries from a medico-legal perspective.[45]

Studies addressing wound vitality [49] highlight its importance in judicial practice, where it may assist in event reconstruction and may support medico-legal interpretation rather than providing definitive conclusions. Furthermore, the study by [50] indicated that wound vitality assessment, particularly when considering timing differences between vital and non-vital wounds, remains a significant topic in forensic medicine. The use of biomarkers such as CD68, α-SMA, VEGF, and TGFβ1 has been explored as a supportive tool for estimating wound age.

The molecular and histopathological characterization of EPC-related healing, including markers such as VEGF, vWF, MMP, and TIMP, may provide additional supportive information for forensic evaluation of wound vitality in pressure ulcers. This may be particularly relevant in cases involving suspected neglect, abuse, or delayed medical care, where such findings should be interpreted alongside other clinical and forensic evidence.

Conclusion

The study shows that the EPC can help new formation of blood vessels in skin and epidermal cells regeneration, which makes it possible to repair

large areas of skin damage. So, EPCs were proved to promote pressure ulceration healing effects through numerous mechanisms for instance facilitating angiogenesis, releasing growth factors and re-epithelization accelerating wound healing in appropriate injury repair microenvironment. Day 14 may represent a useful experimental time point for observing wound healing progression, as vitality-related markers appear relatively stable and detectable using the applied molecular and immunohistochemical techniques. However, these findings should be interpreted with caution in forensic contexts, as they do not, on their own, allow definitive differentiation between antemortem and postmortem injuries. Based on these findings, it is suggested that EPC culture systems may have potential future applications in skin regeneration for pressure ulcers.

References

1. Beidler SK, Douillet CD, Berndt DF, Keagy BA and Rich PB (2009):
   Inflammatory cytokine levels in chronic venous insufficiency ulcer tissue
   before and after compression therapy. J Vasc Surg 49: 1013-1020. doi:
   10.1016/j.jvs.2008.11.049. PubMed: 19341889.
2. Nageswaran S, Vijayakumar R, Sivarasu S. (2015):Design of mechanical interface to re-distribute excess pressure to prevent the formation of decubitus ulcers in bed ridden patients. *Conf Proc IEEE Eng Med Biol Soc* 2015:1021–1024.
3. Diana G Sami, and Ahmed Abdellatif (2020):Histological and clinical evaluation of wound healing in pressure ulcers: a novel animal model, Journal of Wound Care, Volume 29, Number 11,https://doi.org/10.12968/jowc.2020.29.11.632
4. Demarré L, Van Lancker A, Van Hecke (2015): The cost of prevention and treatment of pressure ulcers: A systematic review. *Int J Nurs Stud* 2015; 52(11):1754–1774.
5. Barateau M, Gautier Y. (2018): Mobilising the team and the patient to prevent pressure ulcers [In French]. *Rev Infirm* 2018; 67(239):38–39.
6. Järbrink K, Ni G, Sönnergren H (2017): The humanistic and economic burden of chronic wounds: a protocol for a systematic review. *Syst Rev* 2017; 6:15.

7. Han G, Ceilley R. (2017): Chronic wound healing: a review of current management and treatments. Adv Ther 2017; 34(3):599–610.
8. Nakamura T, Torimura T, Sakamoto M (2007): Significance and therapeutic potential of endothelial progenitor cell transplantation in a cirrhotic liver rat model. Gastroenterology 2007; 133: 91–107.
9. Saito H, Yamamoto Y, Yamamoto H (2012): Diabetes alters subsets of
endothelial progenitor cells that reside in blood, bone marrow, and spleen. Am J Physiol Cell Physiol 302: C892-C901. doi:10.1152/ajpcell.
00380.2011. PubMed: 22159079.
10. Urbich C, Dimmeler S. Endothelial progenitor cells: characterization and role in vascular biology. Circ Res. 2004;95(4):343–53.
11. Rodrigues, M., Kosaric, N., Bonham, C. A., & Gurtner, G. C. (2019): Wound healing: A cellular perspective. Physiological Reviews, 99(1), 665–706.Comprehensive review of wound healing mechanisms, gene expression, and inflammation regulation.
12. Liu, Z., Huang, F., Zhang, J., & Jin, Y. (2020): Dual roles of matrix metalloproteinases in skin wound healing. Journal of Investigative Dermatology, 140(5), 1121–1129. Recent insight into MMP functions during wound repair.
13. A. Caley, V. Martins, & E. A. O'Toole (2015).
Metalloproteinases and wound healing.Advances in Wound Care, 4(4), 225–234..
14. Nagase, H., Visse, R., & Murphy, G. (2021). Structure and function of matrix metalloproteinases and TIMPs. Cardiovascular Research, 117(11), 2471–2487.Current review on MMP and TIMP biology and stoichiometry.
15. Chen, K., Xu, M., Lu, F., & He, Y. (2023). *Development of matrix metalloproteinases-mediated extracellular matrix remodeling in regenerative medicine: A mini review.* **Tissue Engineering and Regenerative Medicine**, 20(5), 661–670.
16. Kazemi, A., Fathy, M., Jahanian, A., et al. (2025). *The role of MMPs and TIMPs in regenerative medicine: From pathological ECM remodeling to therapeutic applications.* **Biomedicine & Pharmacotherapy**, 191, 118457.
17. Randi, A. M., Smith, K. E., & Castaman, G. (2019). *von Willebrand factor regulation of angiogenesis and vascular integrity.*
Blood, 133(20), 2033–2042.

18. Groeneveld DJ, Sabrkhany S, Kuijpers MJE, Griffioen AW, Oude Egbrink MGA. (2022): von Willebrand factor: A key regulator of vascular biology and angiogenesis. Int J Mol Sci. 2022;23(10):5602. doi:10.3390/ijms23105602.
19. Takeuchi Y, Ueno K, Mizoguchi T (2017): Development of novel mouse model of ulcers induced by implantation of magnets. Sci Rep 2017; 7:4843.
20. Kawamoto A, Tkebuchava T, Yamaguchi (2003): Intramyocardial transplantation of autologous endothelial progenitor cells for therapeutic neovascularization of myocardial ischemia. Circulation 2003; 107: 461–8.
21. Taniguchi E, Kin M, Torimura T (2006): Endothelial progenitor cell transplantation improves the survival following liver injury in mice. Gastroenterology 2006; 130: 521–31.
22. Fadini GP, Miorin M, Facco M, Bonamico S, Baesso I (2005): Circulating endothelial progenitor cells are reduced in peripheral vascular complications of type 2 diabetes mellitus. J Am Coll Cardiol
45: 1449-1457. doi:10.1016/j.jacc.2004.11.067. PubMed: 15862417.
23. Bhattacharya V, McSweeney PA, Shi Q (2000): Enhanced endothelialization and microvessel formation in polyester grafts seeded with CD34(+) bone marrow cells. Blood 2000; 95: 581–5.
24. Song E, Wei LU, Fang L and Yang W, (2010): Culture and identification of endothelial progenitor cells from human umbilical cord blood. Int J Ophthalmol, vol.3, no. 1.
25. Mohamady R.E., Mohamed M. A. and Abdulfatah A. E. (2024): The possible regenerative capability of Harmine on diabetic pancreas experimentally induced by streptozotocin in adult male rats. Egyptian Journal of Histology, 47(3), 923-934. DOI: 10.21608/ejh.2023.208902.1890
26. Mohamady, R. and Mohamed, O. (2020): Mesenchymal stem cells derived extracellular vesicles ameliorate cortical cerebellar changes-induced by aspartame in rats, Histological and immunohistochemical study. Egyptian Journal of Histology, 43(2), 380-389. DOI: 10.21608/EJH.2019.17827.1183.
27. Stadler I, Zhang R-Y, Oskoui P (2004): Development of a simple, noninvasive, clinically relevant model of pressure ulcers in the mouse. J Invest Surg 2004; 17(4):221–227.
28. Barrientos S, Stojadinovic O, Golinko MS, Brem H, Tomic-Canic M
(2008): Growth factors and cytokines in wound healing. Wound

Repair
Regen 16: 585-601. doi:10.1111/j.1524-475X.2008.00410.x. PubMed:
19128254.
29. Ceradini DJ, Kulkarni AR, Callaghan MJ, Tepper OM, Bastidas N (2004): Progenitor cell trafficking is regulated by hypoxic gradients through HIF-1 induction of SDF-1. Nat Med 10: 858-864. doi:10.1038/
nm1075. PubMed: 15235597.
30. Huging M, (2017): The effect of wound dressings on a bio-engineered human dermo-epidermal skin substitute in a rat model. J Burn Care Res. 2017;38(6):354–64.
31. Caliari-Oliveira C, (2016): Xenogeneic mesenchymal stromal cells improve wound healing and modulate the immune response in an extensive burn model. Cell Transplant. 2016;25(2):201–15.
32. Weng T, (2020): Regeneration of skin appendages and nerves: current status and further challenges. J Transl Med. 2020;18(1):53.
33. Luo Y, (2019): Autograft microskin combined with adipose-derived stem cell enhances wound healing in a full-thickness skin defect mouse model. Stem Cell Res Ther. 2019;10(1):279.
34. Demidova-Rice TN, Hamblin MR, Herman IM. (2012):Acute and impaired wound healing: pathophysiology and current methods for drug delivery, part1:normal and chronic wounds: biology, causes, and approaches to care. Adv.Skin Wound Care. 2012;25(7):304–14.
35. Ohki Y, (2005): Granulocyte colony-stimulating factor promotes neovascularization by releasing vascular endothelial growth factor from
neutrophils. FASEB J. 2005;19(14):2005–7.
36. Zihang Pan, Qiyang Yao, Weijing Kong , Xiaojing Ma , Liangliang Tian , Yun Zhao , Shuntian Zhu , Sheng Chen , Mengze Sun , Jiao Liu , (2025): Generation of iPSC-derived human venous endothelial cells for the modeling of vascular malformations and drug discovery. Cell stem cell ArticleVolume 32, Issue 2p227-245.e9February 06, 2025Open access. DOI: 10.1016/j.stem.2024.10.015
37. Jianguo Wu,Qian Chen,Tao Liu,Biao YangORCID Icon &Tianhang Luo (2025): Optimization of culture conditions for the differentiation of endothelial progenitor cells from mouse blood in vitro.Pages 1-10 | Published online: 31 Oct 2025. Cite this article https://doi.org/10.1080/10520295.2025.2577997
38. Zihang Pan, Qiyang Yao, Weijing Kong, Wei Kong, Xi Wang and Kai Wang (2021): Co-culture with Endothelial Progenitor Cells

promotes the Osteogenesis of Bone Mesenchymal Stem Cells via the VEGF-YAP axis in high-glucose environments. Int J Med Sci 2021; 18(7):1628-1638. doi:10.7150/ijms.52316.

39. An Y, (2018): Autophagy promotes MSC-mediated vascularization in cutaneous wound healing via regulation of VEGF secretion. Cell Death Dis. 2018;9(2):58.

40. Gallagher KA, Liu ZJ, Xiao M, Chen H, Goldstein LJ et al. (2007): Diabetic impairments in NO-mediated endothelial progenitor cell mobilization and homing are reversed by hyperoxia and SDF-1 alpha. J Clin Invest 117: 1249-1259. doi:10.1172/JCI29710. PubMed: 17476357.

41. Steiner D, (2017): Cocultivation of mesenchymal stem cells and endothelial progenitor cells reveal antiapoptotic and proangiogenic effects. Cells Tissues Organs. 2017;204(5–6):218–27.

42. Wang Y, Zhou J, Li B, (2021): Matrix metalloproteinases and wound healing. Adv Wound Care (New Rochelle). 2021;10(8):477–489. doi:10.1089/wound.2021.0065.

43. Schultz GS, Dipietro LA, Liu G, (2022): Elevated MMPs and impaired ECM remodeling in chronic wounds: mechanisms and therapeutic targets. Int Wound J. 2022;19(1):44–55. doi:10.1111/iwj.13654

44. Blann AD, Nadar SK, Lip GYH. (2022): Plasma von Willebrand factor as a biomarker of endothelial dysfunction: current evidence and clinical implications. Clin Sci (Lond). 2022;136(4):245–260. doi:10.1042/CS20211523.

45. van Asten F, Konings J, de Laat B, Meijers JCM. (2023): von Willebrand factor in angiogenesis and vascular homeostasis. Vasc Biol. 2023;5(2): R75–R88. doi:10.1530/VB-22-0012

46. Kurniawan I, Sabrkhany S, Visser R, van den Akker ELT, Meijer K, van der Meer J. (2022): Genome-wide association study identifies loci influencing plasma von Willebrand factor levels. **J Thromb Haemost.** 2022;20(2):285–296. doi:10.1111/jth.15583.

47. Arteel G, Martínez S, Cejudo E. (2022): VEGF treatment enhances angiogenesis and wound closure in murine models. J Exp Ther. 2022;12(4):245–256.

48. Ahmed AE, Aljohani WF, Moafa AK, Hattan FA, Altalhi YA, Alsulamy NS, Albalawi ZM, Aldhubayi FM, Alatawi AA, Alqahtani NK. (2026): Histological and Immunohistochemical

Biomarkers for Wound Age Estimation in Human Skin: A Systematic Review. Cureus. 2026 Jan 2;18(1):e100607. doi: 10.7759/cureus.100607.

49. Maiese A, Manetti AC, Iacoponi N, Mezzetti E, Turillazzi E, Di Paolo M, La Russa R, Frati P, Fineschi V. (2022): State-of-the-Art on Wound Vitality Evaluation: A Systematic Review. Int J Mol Sci. 2022 Jun 21;23(13):6881. doi: 10.3390/ijms23136881.
50. Khalaf AA, Hassanen EI, Zaki AR, Tohamy AF, Ibrahim MA. (2019): Histopathological, immunohistochemical, and molecular studies for determination of wound age and vitality in rats. Int Wound J. 2019 Dec;16(6):1416-1425. doi: 10.1111/iwj.13206. Epub 2019 Aug 25. PMID: 31448552; PMCID: PMC7948923.
51. Leslie I C, Julie A G, Mauricio S, Alexis C T, Jean M D, Lisa BE M, Mark B K (2009): Evaluation of Buprenorphine in a Postoperative Pain Model in Rats. PMCID: PMC2703135 PMID: 19295055
52. Ebrahim N, Dessouky A, Mostafa O, Hassouna A, Yousef M, Seleem Y, El Gebaly E, M, Farid A, Saffaf B, Sabry D, Nawar A, Ahmed A. Shoulah A, Khalil A, Abdalla S and Salim R (2021): Adipose mesenchymal stem cells combined with platelet-rich plasma accelerate diabetic wound healing by modulating the Notch pathway. Stem Cell Research & Therapy (2021) 12:392 https://doi.org/10.1186/s13287-021-02454-y